Computational Materials Science 203 (2022) 111167

Contents lists available at ScienceDirect

Computational Materials Science

journal homepage: www.elsevier.com/locate/commatsci

# Calibrating the unphysical divergence in TDDFT + U simulations of a correlated oxide

Peiwei You [a,c], Daqiang Chen [a,c], Sheng Meng [a,b,c,*]

[a] Beijing National Laboratory for Condensed Matter Physics and Institute of Physics, Chinese Academy of Sciences, Beijing 100190, China
[b] Songshan Lake Materials Laboratory, Dongguan, Guangdong 523808, China
[c] School of Physical Sciences, University of Chinese Academy of Sciences, Beijing 100049, China

ARTICLE INFO

*Keywords:*
Time dependent density functional theory
TDDFT+U
First-principle nonadiabatic dynamics
Transition metal oxide

ABSTRACT

To simulate the photoexcited molecular dynamics of strongly correlated materials, we implement the Hubbard U term for the proper account of the on-site Coulomb interaction in the real-time time dependent density functional theory (TDDFT + U) molecular dynamics simulations. As a prototype example, we present first-principles simulations of excited state dynamics in a typical transition metal oxide (rutile $TiO_2$) containing d-orbital electrons. We find an unphysical divergence originated from the overcoherence in the evolution of density matrix, which can be alleviated by a diagonalization procedure proposed here. Upon this correction, we identify an intrinsic charge localization dynamics in rutile $TiO_2$ upon photoexcitation, which offers a microscopic understanding of the photoinduced processes in correlated transition metal oxides.

## 1. Introduction

A basic problem in conventional first-principles calculations is the accurate modeling of strongly correlated materials. Without exception, the proper description of the electronic correlation effects in the rapidly developing real-time time dependent density functional theory molecular dynamics (TDDFT-MD) approaches remains a major challenge. Since more and more time-resolved spectroscopies [1–6] in the ultrafast femtosecond timescale have been developed and applied in various research fields, TDDFT-MD, which can provide molecular understanding for the underlying dynamics, is gradually applied to simulate many realistic systems and processes, e.g. charge density wave materials [7,8], ion-beam irradiation [9,10], photocatalytic water splitting [11,12] and magnon dynamics [13]. It is essential to include accurate electron–electron interactions in molecular dynamics simulations when this method is used for some typical d-band correlated materials (such as $TiO_2$ and NiO).

For the ground state calculations, one can adopt the well-established and widely used approximations from the Hubbard model for the exchange and correlation functional, named the DFT + U method. The effective Hubbard U for on-site Coulomb repulsion has been implemented in many ground state softwares [14–16]. Typical values of Hubbard U of different elements can be assessed through linear response calculations [17], and constrained random phase approximation [18,19].

To consider the on-site Coulomb repulsion in the TDDFT framework, we can retain the Hubbard correction, at the same time use the adiabatic approximation to build the exchange and correlation functional. In other words, the exchange and correlation functional has the same form with that in DFT but as a function of electron density at a given moment, written as $V^{XC}(\boldsymbol{r},t)\rightarrow V^{XC}[n(t)](\boldsymbol{r})$. Here $\boldsymbol{r}$, $t$, and $n(t)$ denote electronic coordinates, time, and electronic density, respectively. Although the adiabatic approximation is valid in many excited state dynamics, the drawback of the ground state exchange and correlation functional is inherited at once: the underestimated energy gap and self-interaction error, which may be corrected using Hubbard model. Based on these approximations, the Hubbard term can be evaluated as $V^{Hub}(\boldsymbol{r},t)\rightarrow V^{Hub}[n(t)](\boldsymbol{r})$, namely the TDDFT + U approach. Nicolas and co-workers have investigated the dynamical Hubbard term corresponding to the time dependent electronic density expressed onto real-space grids, finding that electrons excited from the localized subspace to delocalized area can lead to the enhanced screening [20,21].

Here we develop the TDDFT + U framework employing the local atomic basis set, calibrating the applicability of this approach in realistic

* Corresponding author at: Beijing National Laboratory for Condensed Matter Physics and Institute of Physics, Chinese Academy of Sciences, Beijing 100190, China.
*E-mail address:* smeng@iphy.ac.cn (S. Meng).

https://doi.org/10.1016/j.commatsci.2021.111167
Received 27 September 2021; Received in revised form 17 December 2021; Accepted 20 December 2021
Available online 31 December 2021

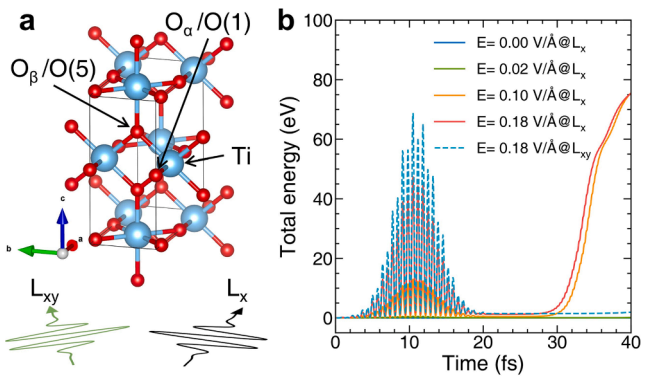


**Fig. 1.** **a**, The supercell of rutile $TiO_2$, containing four Ti atoms (blue) and eight O atoms (red). Two kinds of light field ($L_x$, $L_{xy}$), whose polarizations are along x direction and xy direction of lattice, are applied to manipulate the photoexcitation of rutile $TiO_2$. **b**, The total energy upon different light intensities (E = 0, 0.02, 0.10 and 0.18 V/Å), where the polarization is along x direction.

dynamic simulations of correlated materials. Potentially, the real time evolution of both electronic structure and nuclear dynamics for various strongly correlated materials can be investigated, to address the importance of dynamical information. As a prototype example, the transition metal oxide $TiO_2$ serves as catalytic materials widely adopted in academic research and industrial applications [22–25]. The photoexcited state of $TiO_2$ plays an essential role in the photocatalytic processes. Experiments by the two-photon photoemission (2PPE) have detected the thermalization processes of injected electrons [26], and the resonant excited state derived from $Ti^{3+}$ species [27], exhibiting distinct photoexcitation features in different energy regions. In general, after photoexcitation the photogenerated electrons are trapped on $Ti^{4+}$ while the holes are localized on oxygen atoms, beaconing a microscopic picture for the trapping and relaxation dynamics of hot carriers, nevertheless, with a much speculative nature [28]. The dynamical behavior of electrons, especially the charge localization corresponding to the light-matter interactions, is largely questionable. Therefore, we intend to investigate the dynamic charge transfer behaviors in the rutile $TiO_2$ upon photoexcitation in different light fields, using the TDDFT + U framework.

In this work, we show there is an unphysical divergence of total energy in typical TDDFT + U simulations, in the case of strong excitation. The divergent behavior can be corrected using a diagonalization procedure during the time evolution of Kohn-Sham states. Using the newly developed TDDFT + U approach, we identify the temporal characters of charge localization dynamics upon light stimulation in rutile $TiO_2$, in particular, the real time evolution of real-space distribution of electronic density and occupation of different *3d* orbitals.

## 2. TDDFT + U framework

For the influence of on-stie Hubbard U repulsion on *3d* electrons, the time-dependent Kohn-Sham (TDKS) equation employing numerical atomic orbital basis sets can be written as:

$$i\hbar\frac{\partial}{\partial t}\psi(\boldsymbol{r},t) = \left[-\frac{\nabla^2}{2} + \sum V_I^{local}(\boldsymbol{r}) + \sum V_I^{KB} + V^H(\boldsymbol{r},t) + V^{XC}(\boldsymbol{r},t) + U_{ext}(\boldsymbol{r},\boldsymbol{R},t) + V^{Hub}\right]\psi(\boldsymbol{r},t) \quad (1)$$

where the $V_I^{local}(\boldsymbol{r})$ and $V_I^{KB}$ are the local and Kleinman-Bylander parts of the pseudopotential of atom $I$, while $V^H(\mathbf{r},t)$, $V^{XC}(\mathbf{r},t)$ and $U_{ext}(\boldsymbol{r},\boldsymbol{R},t)$ are the Hartree, exchange–correlation (XC) and external potentials, respectively. The density matrix of Hubbard potential $V^{Hub}$ based on different $d$ orbitals (index $i$ and $j$) and spin index $\sigma$ should be written as [14,20]:

$$V_{ij}^{Hub,\sigma} = U_{eff}\left(\frac{1}{2}\delta_{ij} - \rho_{ij}^{\sigma}\right)\widehat{P}_{ij}^{\sigma} \quad (2)$$

Here the $U_{eff}$ is reformulated by subtracting Hund's $J$ from Hubbard

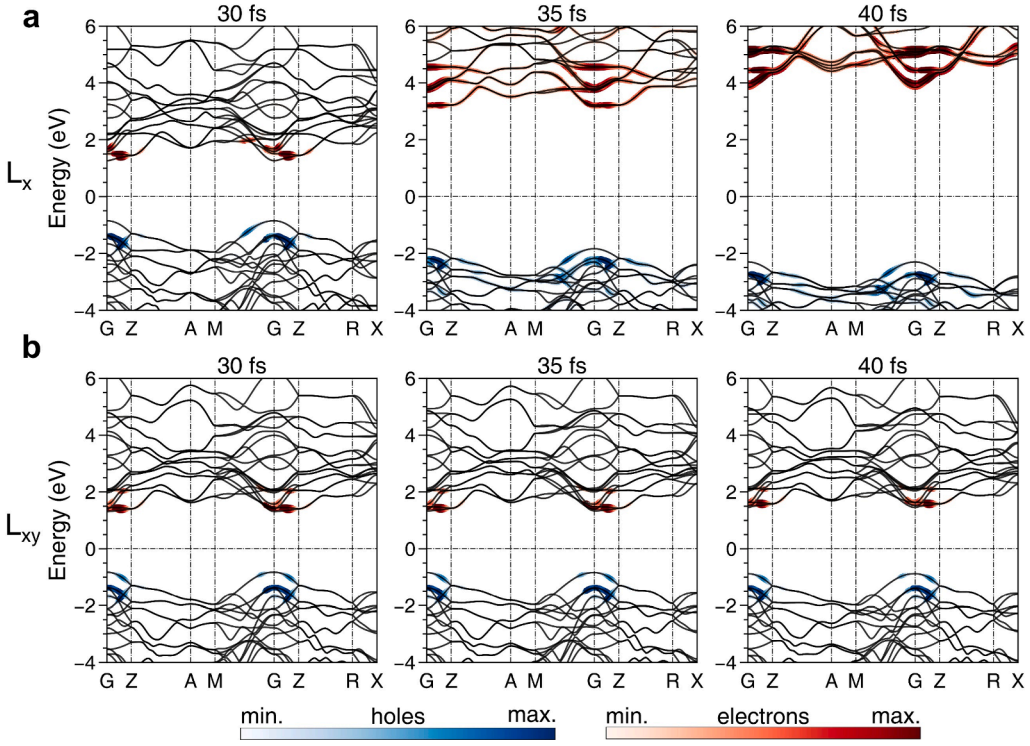


**Fig. 2.** Excited band structure at different typical snapshots (30, 35, 40 fs), under the $L_x$ light field (**a**) and $L_{xy}$ light field (**b**), where the strength of light field is 0.18 V/Å. The population of photogenerated electrons and holes are depicted by the color bar.

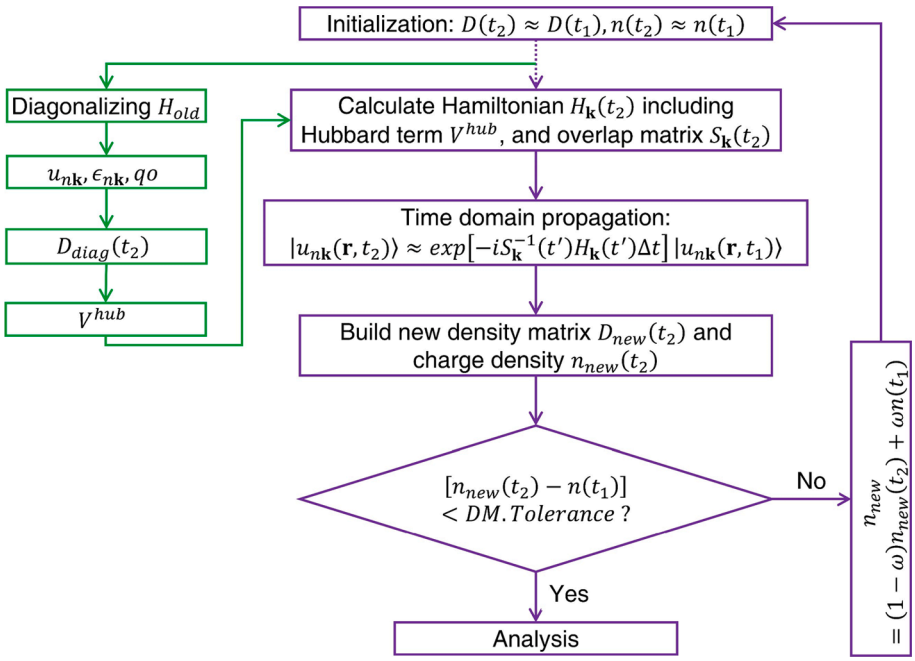


**Fig. 3.** Schematical flowchart of the diagonalization correction, where the time-evolved Hamiltonian is substituted by the diagonalized Hamiltonian when the Hubbard term is evaluated. The rest of calculation processes are preserved. Newly added calculations are denoted as green color.

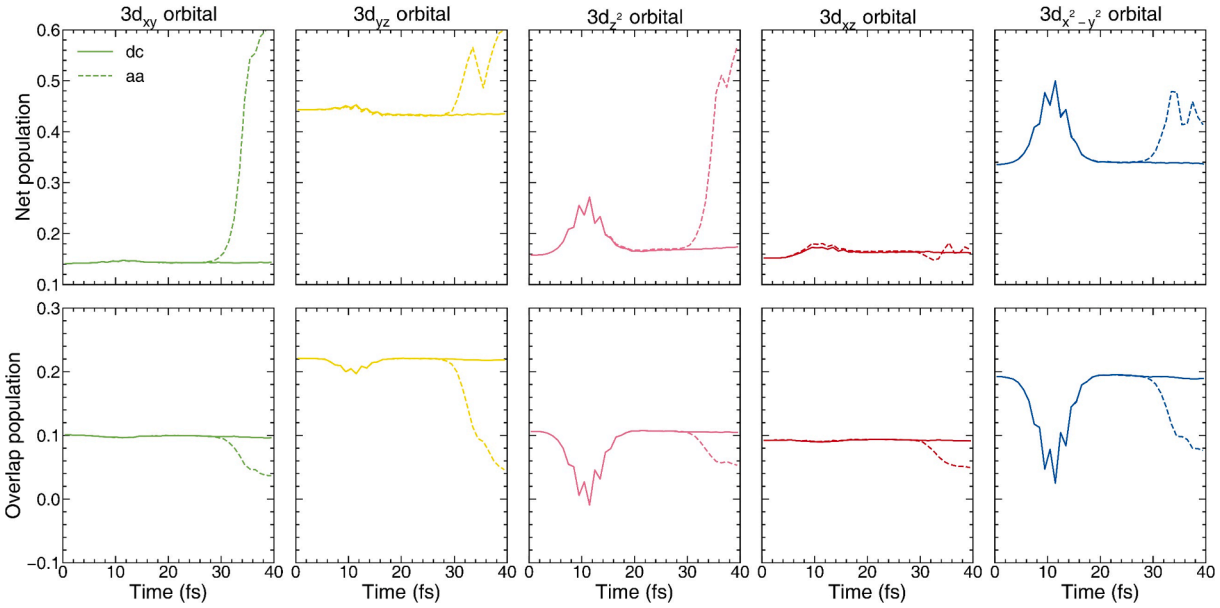


**Fig. 4.** The charge population comparison for all *3d* orbitals of the Ti atom (as labeled in Fig. 1a), where the solid lines and dashed lines denote results with our diagonalized correction (dc) and the original adiabatic approximation (aa), respectively.

$U$. The $\widehat{P}_{ij}^{\sigma} = |\phi_i^{\sigma}\rangle\langle\phi_j^{\sigma}|$ is the projected operator for the subspace localized orbitals. We denote all the terms of electronic Hamiltonian as $H_{ks}$, which includes the original TDDFT part ($H_{tddft}$) and newly added Hubbard term ($V^{Hub}$).

The time propagation operator is constructed using first order Crank–Nicholson scheme:

$$U(t+\Delta t, t) = \frac{S - iH_{ks}\Delta t/2}{S + iH_{ks}\Delta t/2} = \frac{S - iH_{tddft}\Delta t/2 - iV^{Hub}\Delta t/2}{S + iH_{tddft}\Delta t/2 + iV^{Hub}\Delta t/2}, V^{Hub} = U_{eff}\left(\frac{1}{2}\delta - \widehat{\rho}_{sub}\right)\widehat{P}^{\sigma} \quad (3)$$

$$S = \langle\phi_m|\phi_n\rangle \quad (4)$$

where the $\widehat{\rho}_{sub}$ represents local subspace density operator for *3d* electrons. The overlap matrix $S$ can be obtained by multiplication of different orbitals. The time propagation for the TDKS wavefunction $\psi(\mathbf{r}, t)$ is performed as follows:

$$\psi(\mathbf{r}, t+\Delta t) = U(t+\Delta t, t)\psi(\mathbf{r}, t) \quad (5)$$

We note that the modified term directly couples with the time-dependent electronic density at each time step. Once the time propagation operator is obtained, the wavefunction is evolved in real time, and the following molecular dynamics are calculated within the

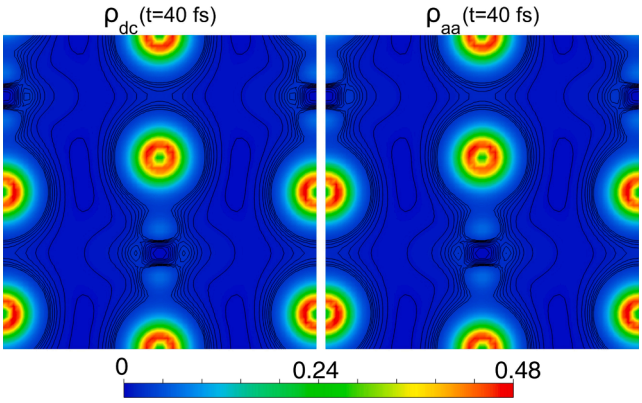


**Fig. 5.** The time dependent electronic density in the (0 1 0) plane of $TiO_2$ comprising oxygen atoms at 40 fs after photoexcitation, using both the diagonalization correction ($\rho_{dc}$) and adiabatic approximation ($\rho_{aa}$). The contour lines start from zero, with an interval of 0.003. All the unit of electronic density is 1 e/Bohr$^3$.

Ehrenfest scheme.

## 3. Photoexcitation analysis

The rutile $TiO_2$ is modeled by a supercell in Fig. 1a, consisting of total 12 atoms. We sample the Brillouin zone by 4 × 8 × 4 k points and optimize the supercell where the lattice constants are a = c = 6.57 Å and b = 2.99 Å. The TDDFT-MD is performed by the time-dependent ab initio package (TDAP) [29–31], and the time-dependent Kohn-Sham wavefunctions under light fields are evolved for 800 steps with a time step of 50 attoseconds (Δt = 0.05 fs) using the constant-energy ensemble (NVE). The value of mixing weight for density matrix in electronic self-consistency is 0.05. A benchmark calculation with Δt = 0.01 fs is presented in supplement Figure S1. The energy cutoff of 200 Ry is used and the Hubbard *U* value is 4.2 eV [32]. The light field with a photon energy of 3.1 eV is chosen, and the full width at half maximum (FWHM) is 8 fs. Two polarizations of light fields, in the x direction and diagonal xy direction of lattice ($L_x$, $L_{xy}$), respectively, are chosen.

Firstly, we show that the unphysical divergence of total energy shows up under strong excitations. In response to the strong light field (E > 0.10 V/Å) where the polarization is along with x direction (labeled as $L_x$), the total energy of the system presented in Fig. 1b shows a rapid increase after 30 fs while the temperature has no apparent change, indicating the electronic structure goes divergent. In principle, the total energy should be a constant using the constant-energy ensemble when the light field is off. In the weak excited state (E = 0.02 V/Å), the system maintains a good stability due to the fact that only a very small fraction of electrons is excited. For comparison, the light fields with $L_{xy}$ polarization do not trigger the divergence of total energy surprisingly.

To check the divergence of the electronic structure (under the laser field of E = 0.18 V/Å, $L_x$), we calculate the time resolved band structure at 30, 35, 40 fs via the projection from TDKS orbitals to adiabatic states [33], as shown in Fig. 2a. With the time flow (30 ~ 40 fs), the conduction bands are repulsed upward while the valence bands fall into deeper energy levels, accompanied with the large increase of excited carriers along the whole high symmetric k paths. At last, the band structure is fully destroyed. The largest population is near the gamma point, where ~ 2 $e^-$ are excited from the valence bands. The band structure under the intensity E = 0.02 V/Å is always stable, where the population at gamma point is as small as ~ 0.1 $e^-$, consistent with the small population in bulk NiO presented in Ref [21]. In contrast, the excited band structure (E = 0.18 V/Å, $L_{xy}$) in Fig. 2b is well maintained, resulting in no divergence.

The analysis implies the time propagation error in TDDFT + U can be amplified by strong light irradiation, and fails to describe the system properly in the case of selective excitation modes. Since time propagation is directly coupled to the time-dependent electronic density at each time step, the numerical instability can be ascribed to two reasons: i) the nonsymmetric excitation causes wrong overcoherence in the density matrix of excited electrons between *3d* orbitals and other atomic orbitals (e. g. *2p* orbitals of oxygen atoms), which triggers unphysical increase of Hubbard energy; and ii) the time step is too large. The convergence was nicely achieved in Shin et al.'s scheme, where a tiny time step (dt = 0.0048 fs) is used within the Suzuki − Trotter splitting and Crank − Nicolson scheme [34]. Besides, the excited state generated by alkali atoms attack in Ref. [34] may be close to the equilibrium state, which is different from the present case of strong photoexcitations (~2 electrons promoted) far away from the equilibrium. We also simulate the TDDFT + U dynamics under strong photoexcitation using time dependent ab initio code (TDAPW) [31] with a more accurate propagation algorithm (Figure S2). The time propagation errors diminish, indicating an improved algorithm of time evolution operator might be helpful to solve the numerical instability. Although in this simple model the unphysical divergence can be relieved using Δt = 0.01 fs, as shown in supplementary Figure S1, this procedure cannot always work in complex systems (e. g. $H_2O/TiO_2$ interface, $O_2/TiO_2$ interface), where fast charge flow may lead to wrong dynamics (Figure S3). To deal with the divergent error of photoexcitation while using a large time step, we propose an alternative method, namely, the diagonalization correction.

## 4. Diagonalization correction

Using a short time step can partly tackle the numerical instability but it is too time consuming for large systems, neither does it guarantee the accuracy. Here we propose the diagonalization approach to correct approximately the overcoherence of excited electronic density, providing a stable time propagation formulation.

The key consideration is to correctly calculate the time-dependent Hubbard term in the TDDFT framework. Within the first-principles framework, the Hubbard term can be regarded as a penalty functional to reduce the self-interaction error in the first-order perturbation, determining the energy level of unoccupied state above the Fermi level in such a way. One can obtain the Hubbard *U* value by the change of the *3d* energy level when the occupation of localized *3d* electrons is varied [35]. We keep the basic idea that the Hubbard term can be regarded as a penalty functional in the TDDFT framework, thus we can approximate the penalty functional using the adiabatic wavefunctions on the fly from the time-evolved density, instead of directly using the time-dependent Kohn-Sham orbitals. The occupation is set as that electrons fill in the orbitals below the Fermi level, and the off-diagonal elements in the Hubbard term originated from excited occupation can be eliminated. In principle, this approach is able to produce a correct electronic band structure with a proper Hubbard repulsion, and yields identical trajectories to those from more accurate calculations when performing molecular dynamics with TDDFT + U. The extra repulsion arising from excited electrons might be included in a dynamically modulated Hubbard *U* value [21].

The flowchart for calculating the Hubbard term in the modified TDDFT + U framework is presented in Fig. 3. By diagonalizing the Hamiltonian from the former timestep, we obtain the adiabatic eigenstates and eigenvalues of time dependent electronic structure. These adiabatic wavefunctions, with all the electrons occupied below the Fermi level, can been reformulated into a new diagonalized density matrix. Then we rebuild the time dependent Hubbard term using the new density matrix $V^{Hub}(\boldsymbol{r},t)\rightarrow V^{Hub}\left[n_{diag}(t)\right](\boldsymbol{r})$. The rest part of time dependent formulas and flowchart is unchanged. The original scheme using time-dependent Kohn-Sham wavefunction is depicted as the adiabatic approximation scheme. Both adiabatic scheme (violet color box in Fig. 3) and diagonalization scheme (violet and green color box in Fig. 3) go through the self-consistent calculation. The adiabatic scheme

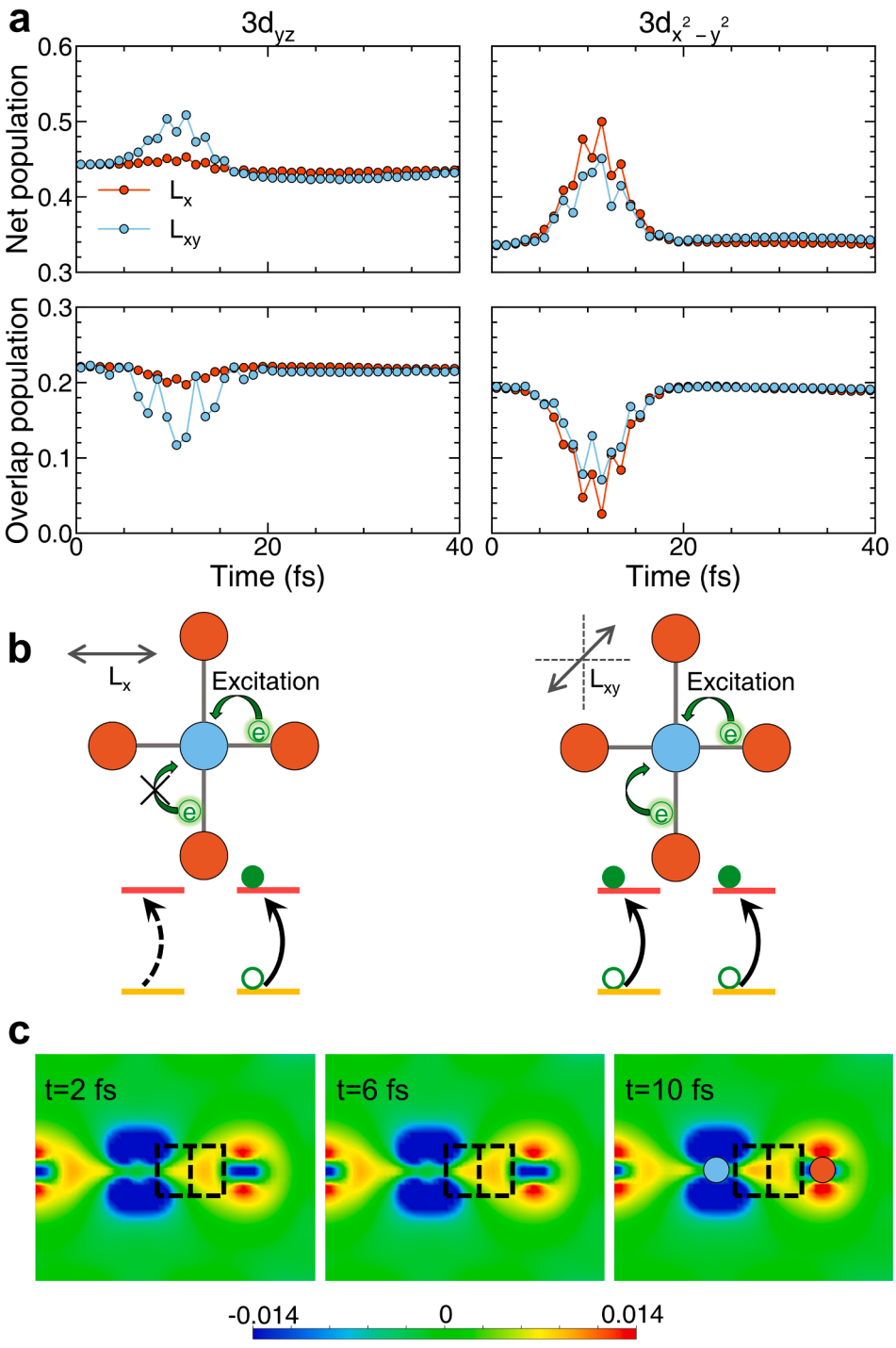


**Fig. 6.** **a,** Time-resolved net population for one Ti atom's $3d_{yz}$ orbital and $3d_{x^2-y^2}$ orbital (upper panels) and overlap population (lower panels), obtained from Mulliken charge analysis. The results with respect to $L_x$ and $L_{xy}$ are denoted by orange and blue lines, respectively. **b**, Schematic pictures for the photoinduced excitation under different polarized light fields. Green, blue and orange circles depict electrons, Ti atoms and O atoms, respectively. **c**, The 2D (0 1 0) plane of excited differential electronic density ($\Delta\rho = \rho(t) - \rho_{atom}$) at 2,6,10 fs, adopting the diagonalization correction in $L_x$ light. All the unit of electronic density is $1e/Bohr^3$.

adopting predictor–corrector implementation cannot deal with the numerical instability. The computational cost of using diagonalization procedure ($\Delta t = 0.05$ fs) and adiabatic approximation ($\Delta t = 0.01$ fs) is nearly the same, which is also three times longer than that using adiabatic approximation with a large time step ($\Delta t = 0.05$ fs). The additional time cost comes from the recalculated density matrixes and extra self-consistent electronic calculations. We also note that the consistence of adiabatic approximation, where all functionals are based on time-dependent electronic density and time-dependent Kohn-Sham wavefunction, is broken in the modified TDDFT + U scheme. This can be justified by the fact that the Hubbard term can be treated as a penalty function in practical calculations.

We then track the Hubbard energy defined as $E^{Hub} = \frac{U_{eff}}{2}\sum_{m,\sigma}[n_{m,\sigma}(t) - n^2_{m,\sigma}(t)]$, which is added to the total energy [14,20], using different Hubbard $U$ values (see Figure S4). Adopting the original adiabatic approximation with a large time step, the Hubbard energy divergence is found after the light irradiation, with a relatively large oscillation caused by the amplified overcoherence from nonsymmetric excitation. Obviously, our diagonalization correction produces the converged Hubbard energy as well as the total energy, which can solve the divergent problem even when a large time step is used. As shown in Fig. 4 and Figure S5, the detailed electronic structure, including the charge localization and band structure, can be corrected by the diagonalization procedure. Before the obvious divergence behavior occurs,

the results using both adiabatic and diagonalization approximation are indeed consistent to each other. In the divergent region, the difference in the population of *3d* electrons demonstrates this correction scheme is effective to eliminate the energy divergence. We note that the total energy is still convergent in a longer-time molecular dynamics as shown in Figure S6.

The validation can be further corroborated through comparing the electronic densities using diagonalization correction with a large time step ($\Delta t = 0.05$ fs) and the adiabatic approximation with a small time step ($\Delta t = 0.01$ fs). In Fig. 5, we present the time dependent electronic density in the photoexcited $TiO_2$ at 40 fs, where the distribution is nearly the same. Besides, the population of excited *3d* electrons is also consistent with each other during the whole propagation process, indicating this diagonalization approach can reproduce the accurate results while using a large time step.

## 5. Charge localization

Using the diagonalization correction method to propagate the time-resolved electronic wavefunctions, we provide the simulated charge localization dynamics between different orbitals upon the illumination of light fields. We separate the Mulliken charge population into the net population and overlap population. The net population can be regarded as all the localized electrons and the overlap population contains unclear occupation with other orbitals. The overlap population is summed over the population between *3d* orbital with the rest atomic orbitals. We focus on the typical Ti (labeled in Fig. 1a) atom's population of $3d_{yz}$ orbital and $3d_{x^2-y^2}$ orbital in Fig. 6a. In the photoexcited period ($0 \sim 20$ fs), the obvious difference is that in $L_x$ light field the net population of $3d_{yz}$ orbital is nearly not excited, so does the overlap population, compared with the situation of $L_{xy}$ light field. This selective orbital excitation can be ascribed to directional Ti-O bonding regions. There are two types of oxygen atoms ($O_\alpha$ and $O_\beta$) in the response of light field, representatively labeled as O(1) and O(5) in Fig. 1a, respectively. In supplementary Figure S7, we specify the difference of photoexcitation originates from the electronic distribution in the bonding region of Ti-O (5) (overlap of $3d_{yz} - 2s$ and $3d_{yz} - 2p_y$ orbitals). A general Hirshfeld charge in Figure S8 also supports that β-type oxygen atoms are not fully excited upon $L_x$ light field, at variance with that in $L_{xy}$ light field. Summarizing the photoexcited charge localization in Fig. 6b, the $L_{xy}$ light field can motivate electrons in two bonding regions to *3d* orbitals, while the $L_x$ light field can not lead to the excitation for one of the two bonding regions, to the $3d_{yz}$ orbital.

The corresponding real-space differential electronic density in the dynamical simulations, with the real-time electronic density minuses the atomic electronic density, is presented in Fig. 6c. Obviously, with the time evolving during $2 \sim 10$ fs, the electrons near the oxygen atoms are moving towards the titanium atom, illustrating the charge localization processes of the *3d* orbitals upon photoexcitation.

## 6. Discussion

We establish a modified TDDFT + U framework based on numerical atomic orbitals and calibrate the unphysical divergence in TDDFT + U simulations of rutile $TiO_2$ upon photoexcitation, originated from the strong population of excited electronic density on different *3d* orbitals and the numerical instability due to the use of a large time step. To stabilize and rationalize the unphysical divergence, we rebuild the Hubbard penalty term adopting a new diagonalization correction, where the adiabatic wavefunctions on the fly are calculated. This approach can reproduce the accurate electronic structures, identifying the selective orbital excitation under different polarization of light fields. The electronic transitions come from the delocalized area to localized subspace (*p* to *d* transition), different from the photoexcitation situations (*d* to *p* transition) in Ref. [21]. While considering the dynamically attenuated screening, the Hubbard *U* value should increase and result in a divergent electronic structure. Therefore, we preserve the further consideration of dynamic screening in the future work, and tackle the precise evolution of electronic density to solve the energy divergence. These results also indicate the nontrivial excited electronic density manipulation when applying the well-defined Hubbard model or GW methods into TDDFT framework. Further molecular dynamics simulations of strongly correlated materials can be performed using the advanced TDDFT + U framework.

## Data availability

The data that support the findings of this study are available from the corresponding authors on reasonable request.

### *CRediT authorship contribution statement*

**Peiwei You:** Conceptualization, Formal analysis, Investigation, Methodology, Software, Visualization, Writing – original draft. **Daqiang Chen:** Software. **Sheng Meng:** Formal analysis, Project administration, Resources, Supervision, Validation, Writing – review & editing.

## Declaration of Competing Interest

The authors declare that they have no known competing financial interests or personal relationships that could have appeared to influence the work reported in this paper.

## Acknowledgements

We acknowledge financial support from MOST (Grant Nos. 2021YFA1400201), NSFC (Grant Nos. 12025407, 11934003, 91850120, and 11774396), and "Strategic Priority Research Program B" of the CAS (No. XDB330301).

## Appendix A. Supplementary material

Supplementary data to this article can be found online at https://doi.org/10.1016/j.commatsci.2021.111167.

## References

[1] B. Dereka, Q. Yu, N.H.C. Lewis, W.B. Carpenter, J.M. Bowman, A. Tokmakoff, Crossover from hydrogen to chemical bonding, Science 371 (2021) 160.
[2] C.W. Nicholson, M. Puppin, A. Lücke, U. Gerstmann, M. Krenz, W.G. Schmidt, L. Rettig, R. Ernstorfer, M. Wolf, Excited-state band mapping and momentum-resolved ultrafast population dynamics in In/Si(111) nanowires investigated with XUV-based time- and angle-resolved photoemission spectroscopy, Phys. Rev. B 99 (15) (2019), https://doi.org/10.1103/PhysRevB.99.155107.
[3] C.W. Nicholson, A. Lücke, W.G. Schmidt, M. Puppin, L. Rettig, R. Ernstorfer, M. Wolf, Beyond the molecular movie: Dynamics of bands and bonds during a photoinduced phase transition, Science 362 (2018) 821.
[4] X. Fu, F. Barantani, S. Gargiulo, I. Madan, G. Berruto, T. LaGrange, L. Jin, J. Wu, G. M. Vanacore, F. Carbone, Y. Zhu, Nanoscale-femtosecond dielectric response of Mott insulators captured by two-color near-field ultrafast electron microscopy, Nat. Commun. 11 (2020) 5770.
[5] G. Rohde, A. Stange, A. Muller, M. Behrendt, L.P. Oloff, K. Hanff, T.J. Albert, P. Hein, K. Rossnagel, M. Bauer, Ultrafast Formation of a Fermi-Dirac Distributed Electron Gas, Phys. Rev. Lett. 121 (2018), 256401.
[6] L.M. Carneiro, S.K. Cushing, C. Liu, Y. Su, P. Yang, A.P. Alivisatos, S.R. Leone, Excitation-wavelength-dependent small polaron trapping of photoexcited carriers in alpha-$Fe_2O_3$, Nat. Mater. 16 (2017) 819–825.
[7] J. Zhang, C. Lian, M. Guan, W. Ma, H. Fu, H. Guo, S. Meng, Photoexcitation Induced Quantum Dynamics of Charge Density Wave and Emergence of a Collective Mode in 1T-$TaS_2$, Nano Lett. 19 (2019) 6027–6034.
[8] C. Lian, S.J. Zhang, S.Q. Hu, M.X. Guan, S. Meng, Ultrafast charge ordering by self-amplified exciton-phonon dynamics in $TiSe_2$, Nat. Commun. 11 (2020) 43.
[9] A.V. Krasheninnikov, Y. Miyamoto, D. Tomanek, Role of electronic excitations in ion collisions with carbon nanostructures, Phys. Rev. Lett. 99 (2007), 016104.
[10] W. He, C. Chen, Z. Xu, Electronic excitation in graphene under single-particle irradiation, Nanotechnology 32 (2021), 165702.
[11] L. Yan, J. Xu, F. Wang, S. Meng, Plasmon-Induced Ultrafast Hydrogen Production in Liquid Water, J. Phys. Chem. Lett. 9 (1) (2018) 63–69.

[12] P. You, C. Lian, D. Chen, J. Xu, C. Zhang, S. Meng, E. Wang, Nonadiabatic Dynamics of Photocatalytic Water Splitting on A Polymeric Semiconductor, Nano Lett. 21 (15) (2021) 6449–6455.
[13] N. Tancogne-Dejean, F.G. Eich, A. Rubio, Time-Dependent Magnons from First Principles, J. Chem. Theory Comput. 16 (2) (2020) 1007–1017.
[14] S.L. Dudarev, G.A. Botton, S.Y. Savrasov, C.J. Humphreys, A.P. Sutton, Electron-energy-loss spectra and the structural stability of nickel oxide: An LSDA+U study, Phys. Rev. B 57 (1998) 1505–1509.
[15] A.B. Shick, A.I. Liechtenstein, W.E. Pickett, Implementation of the LDA+U method using the full-potential linearized augmented plane-wave basis, Phys. Rev. B 60 (15) (1999) 10763–10769.
[16] A. Garcia, N. Papior, A. Akhtar, E. Artacho, V. Blum, E. Bosoni, P. Brandimarte, M. Brandbyge, J.I. Cerda, F. Corsetti, R. Cuadrado, V. Dikan, J. Ferrer, J. Gale, P. Garcia-Fernandez, V.M. Garcia-Suarez, S. Garcia, G. Huhs, S. Illera, R. Korytar, P. Koval, I. Lebedeva, L. Lin, P. Lopez-Tarifa, S.G. Mayo, S. Mohr, P. Ordejon, A. Postnikov, Y. Pouillon, M. Pruneda, R. Robles, D. Sanchez-Portal, J.M. Soler, R. Ullah, V.W. Yu, J. Junquera, Siesta: Recent developments and applications, J. Chem. Phys. 152 (2020), 204108.
[17] M. Cococcioni, S. de Gironcoli, Linear response approach to the calculation of the effective interaction parameters in the LDA+U method, Phys. Rev. B 71 (2005).
[18] F. Aryasetiawan, M. Imada, A. Georges, G. Kotliar, S. Biermann, A.I. Lichtenstein, Frequency-dependent local interactions and low-energy effective models from electronic structure calculations, Phys. Rev. B 70 (19) (2004), https://doi.org/10.1103/PhysRevB.70.195104.
[19] M. Springer, F. Aryasetiawan, Frequency-dependent screened interaction in Ni within the random-phase approximation, Phys. Rev. B 57 (1998) 4364–4368.
[20] N. Tancogne-Dejean, M.J.T. Oliveira, A. Rubio, Self-consistent DFT+U method for real-space time-dependent density functional theory calculations, Phys. Rev. B 96 (2017).
[21] N. Tancogne-Dejean, M.A. Sentef, A. Rubio, Ultrafast Modification of Hubbard U in a Strongly Correlated Material: Ab initio High-Harmonic Generation in NiO, Phys. Rev. Lett. 121 (2018), 097402.
[22] A. Fujishima, X. Zhang, D. Tryk, $TiO_2$ photocatalysis and related surface phenomena, Surf. Sci. Rep. 63 (2008) 515–582.
[23] K. Bourikas, C. Kordulis, A. Lycourghiotis, Titanium dioxide (anatase and rutile): surface chemistry, liquid-solid interface chemistry, and scientific synthesis of supported catalysts, Chem. Rev. 114 (2014) 9754–9823.
[24] J. Schneider, M. Matsuoka, M. Takeuchi, J. Zhang, Y. Horiuchi, M. Anpo, D. W. Bahnemann, Understanding $TiO_2$ photocatalysis: mechanisms and materials, Chem. Rev. 114 (2014) 9919–9986.
[25] Q. Guo, C. Zhou, Z. Ma, X. Yang, Fundamentals of $TiO_2$ Photocatalysis: Concepts, Mechanisms, and Challenges, Adv. Mater. 31 (50) (2019) 1901997, https://doi.org/10.1002/adma.v31.5010.1002/adma.201901997.
[26] L. Gundlach, R. Ernstorfer, F. Willig, Escape dynamics of photoexcited electrons at catechol:$TiO_2$(110), Phys. Rev. B 74 (2006).
[27] Z. Wang, B. Wen, Q. Hao, L.M. Liu, C. Zhou, X. Mao, X. Lang, W.J. Yin, D. Dai, A. Selloni, X. Yang, Localized Excitation of $Ti^{3+}$ Ions in the Photoabsorption and Photocatalytic Activity of Reduced Rutile $TiO_2$, J Am Chem Soc 137 (2015) 9146–9152.
[28] Y. Tamaki, K. Hara, R. Katoh, M. Tachiya, A. Furube, Femtosecond Visible-to-IR Spectroscopy of $TiO_2$ Nanocrystalline Films: Elucidation of the Electron Mobility before Deep Trapping, J. Phys. Chem. C 113 (2009) 11741–11746.
[29] S. Meng, E. Kaxiras, Real-time, local basis-set implementation of time-dependent density functional theory for excited state dynamics simulations, J. Chem. Phys. 129 (2008), 054110.
[30] C. Lian, M. Guan, S. Hu, J. Zhang, S. Meng, Photoexcitation in Solids: First-Principles Quantum Simulations by Real-Time TDDFT, Adv. Theory Simul. 1 (2018) 1800055.
[31] P. You, D. Chen, C. Lian, C. Zhang, S. Meng, First-principles dynamics of photoexcited molecules and materials towards a quantum description, WIREs Comput Mol Sci., DOI 10.1002/wcms.1492(2020) e1492.
[32] P.M. Kowalski, M.F. Camellone, N.N. Nair, B. Meyer, D. Marx, Charge Localization Dynamics Induced by Oxygen Vacancies on the $TiO_2$(110) Surface, Phys. Rev. Lett. 105 (2010).
[33] C. Lian, S.Q. Hu, M.X. Guan, S. Meng, Momentum-resolved TDDFT algorithm in atomic basis for real time tracking of electronic excitation, J. Chem. Phys. 149 (2018), 154104.
[34] D. Shin, G. Lee, Y. Miyamoto, N. Park, Real-Time Propagation via Time-Dependent Density Functional Theory Plus the Hubbard U Potential for Electron-Atom Coupled Dynamics Involving Charge Transfer, J. Chem. Theory Comput. 12 (2016) 201–208.
[35] F. Aryasetiawan, K. Karlsson, O. Jepsen, U. Schönberger, Calculations of Hubbard U from first-principles, Phys. Rev. B 74 (2006).